A coupled model of heat spreading and flow boiling in microchannels

R. Betsema and C.M. Rops
TNO, Nano instrumentation,
High Tech Campus 25, 5656 AE Eindhoven, The Netherlands
e-mail: ruben.betsema@tno.nl and cor.rops@tno.nl

The increasing waste heat density of chips requires advanced cooling technologies to prevent the chip from overheating. Two phase cooling in microchannels with a pin fin structure is a promising method which can extract high heat fluxes with a relatively low pressure drop. Current models to predict the performance of these devices typically assume a uniform heat flux along the flow direction. However, the local heat flux strongly depends on the local properties of the fluid and the local temperature in the adjacent heat spreader. This paper presents a novel model which couples a 2D analytical temperature field to a flow boiling model to obtain an accurate prediction of the boiling process and the maximum temperature at the chip interface. The effectiveness of the coupled model is demonstrated by an optimization study, which shows the sensitivity of design parameters on the maximum temperature.

1. Introduction

The increasing number of transistors per unit area chip gives rise to an increasing waste heat flux density produced by chips [1]. Therefore, a high junction temperature or a non-homogenous distribution of temperature is one of the most common causes of malfunction or shortened lifetime of the chip [2]. Advanced cooling technologies are required which can deal with the increasing heat flux densities and prevent the chip from overheating. Advanced cooling technologies involve liquid cooling in microchannels, flow boiling in microchannels, immersion cooling, impinging jet cooling and spray cooling [3].

Within this paper, flow boiling in microchannels is considered. With this technology, high heat loads can be absorbed with a low flowrate and a compact design. A common problem in microfluidic flow boiling devices is the occurrence of boiling instabilities, leading to low heat transfer and high pressure fluctuations [4]. To mitigate this problem, TNO developed a staggered pin structure which can achieve cooling capacities in the order of ~250W/cm^2 with a relatively low steady pressure drop [5]. Therefore, a complex hierarchical supply and outflow channel, typically seen in literature [6], is not required. In order to design a high-performance microchannel flow boiling cooling device, proper flow boiling models for microchannels are essential.

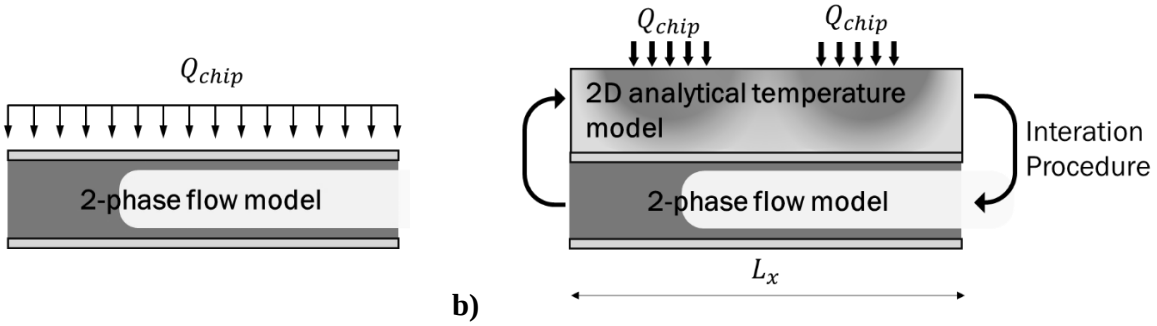

Figure 1. Schematics of flow boiling models: **a)** A fixed uniform heatflux cooled by a two phase flow. **b)** The coupled model for heat spreading and flow boiling.

In a typical microchannel flow boiling device, the heat of the chip is first spread by a heat spreader to reduce the heat flux density before it is absorbed by the cooling fluid [6]. Existing models to predict the temperature of the chip do not take into account the heat spreading (Figure 1a) [7, 8]. The heat flux is assumed to be constant over the length of the channel and the junction temperature is calculated subsequently, using a 1D thermal resistance model. This constant heat flux assumption, is inaccurate as the heat flux is a function of both the temperature of the heat spreader and the local properties of the fluid. In addition, the 1D thermal resistance model underpredicts the maximum temperature as lateral conduction is neglected. In order to take the 2D heat spreading into account, a novel model is developed; Coupling a 2D temperature model to a micro channel flow boiling model (Figure 1b). This coupled model can be used as a design tool to optimize the dimensions of the cooling device to prevent hot spots or high peak temperatures. Furthermore, the model can be extended to more complex designs involving a design containing multiple layers with different thermal conductivities.

2. Coupled 2D temperature and flow boiling model

2.1 Thermal model

The 2D temperature field in the heat spreader can be described by a Fourier series [9]:

$$T(x,y) = C_1 + C_2 y + \sum_{n=0}^{n=\infty} \left(C_3 \sinh\left(\frac{n\pi}{L_x} y\right) + C_4 \cosh\left(\frac{n\pi}{L_x} y\right) \right) \cos\left(\frac{n\pi}{L_x} x\right). \qquad (1)$$

Where, L_x is the width of the heat spreader. The coefficients C_1, C_2, C_3 and C_4 are found using the heat flux profiles at the top and the bottom of the heat spreader, and the inlet temperature of the cooling fluid.

A comparison between the classical 1D thermal resistance model and the 2D approach to model the temperature in the heat spreader is performed by calculating the temperature field inside a 4mm wide block (Figure 2). A 1mm wide heat source with a heat flux density of 250W/cm^2 is used as a boundary condition on top of the domain. In Figure 2b, the resulting temperature profile at the centreline of the domain is shown. This plot clearly shows, that the 1D model significantly underestimates the temperature near the chip.

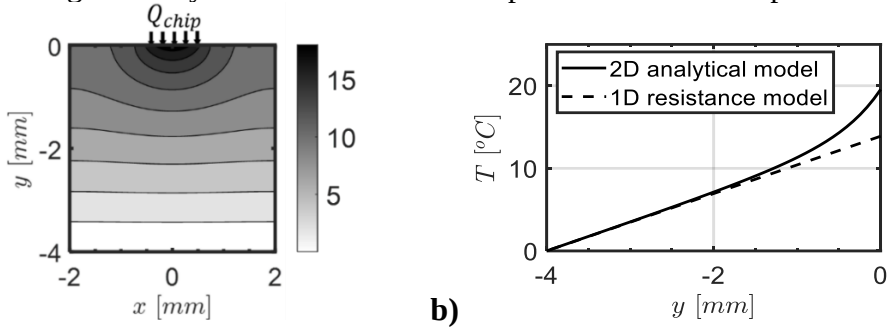

Figure 2. a) The 2D temperature field of a 1mm wide chip on a 4mm wide block, calculated using equation 1. **b)** The 2D analytical model at x = 0mm compared to a 1D resistance model.

2.2 Flow boiling model

To predict the overall cooling performance of the device, the flow behaviour of the cooling fluid is simulated along the length of the channel by a flow boiling model. This model determines the local heat flux from the heat spreader, $q_{spreader}$, into the cooling fluid and the Temperature of cooling fluid, $T_{spreader}$, along the flow direction of the channel. These are the required boundary conditions for the heat spreader model.

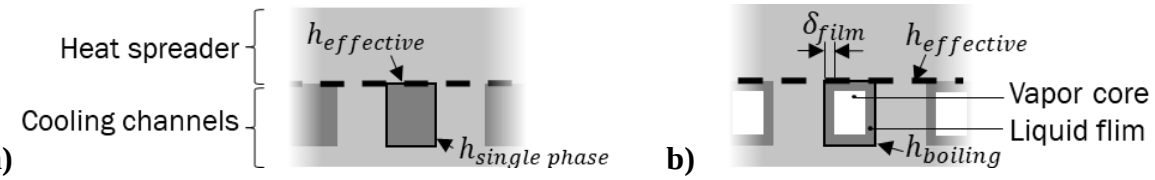

Figure 3. A cross section of the cooling device depicting the plane at which the effective heat transfer coefficient, $h_{effective}$, is assumed. Two different flow regimes: **a)** Single phase flow. **b)** Annular flow boiling.

In the flow boiling model, it is assumed that the flow can be divided into two regimes: single phase flow (Figure 3a) and annular flow boiling (Figure 3b). In the single phase regime, the local heat transfer coefficient, $h_{single\ phase}$, is determined by a Nusselt relation for rectangular channels [10]. In the annular flow boiling regime the heat transfer coefficient, $h_{boiling}$, is determined by the thermal conduction through the liquid film. The thickness of this film is determined by assuming that the shear stress in the liquid film is equal to the shear stress in the vapor core [8]. Furthermore, it is assumed that the channel walls act as fins and its enhancing effect on the heat transfer can be described by a fin formula [10]. The heat flux from the heat spreader into the cooling fluid is given by:

$$q_{spreader}(x) = h_{effective}(x)\left(T_{spreader}(x) - T_{fluid}(x)\right). \quad (2)$$

Where $T_{spreader}(x)$ is the temperature profile at the bottom of the heat spreader, $h_{effective}$, the effective fin heat transfer coefficient and $T_{fluid}(x)$ is the fluid temperature. The two unknown variables $T_{spreader}(x)$ and $q_{spreader}$ are determined by coupling this boiling model to the earlier described heat spreader model.

3. Results and discussion

As an example of a typical use case of the above presented coupled model, two chips of 3mm wide are considered on top of a 15mm heat spreader, each generating a heat flux of 250W/cm^2. The thickness of the heat spreader is set to be 1mm and the width and hight of the channels are set to 0.25mm and 1.0mm respectively. The resulting temperatures are plotted in Figure 4a. The fluid enters as single phase at 80°C and the temperature rises until it reaches the boiling temperature (x ≈ 3mm). The peak temperatures at the top of the heat spreader are 140°C and 130°C respectively and are located at the chip interfaces. The difference in temperature is caused by the change in effective heat transfer coefficient (Figure 4b). For single phase, the heat flux is limited to ~30 kW/m^2 K. In the boiling regime, a significant increase is observed to a heat flux of ~50-100 kW/m^2 K.

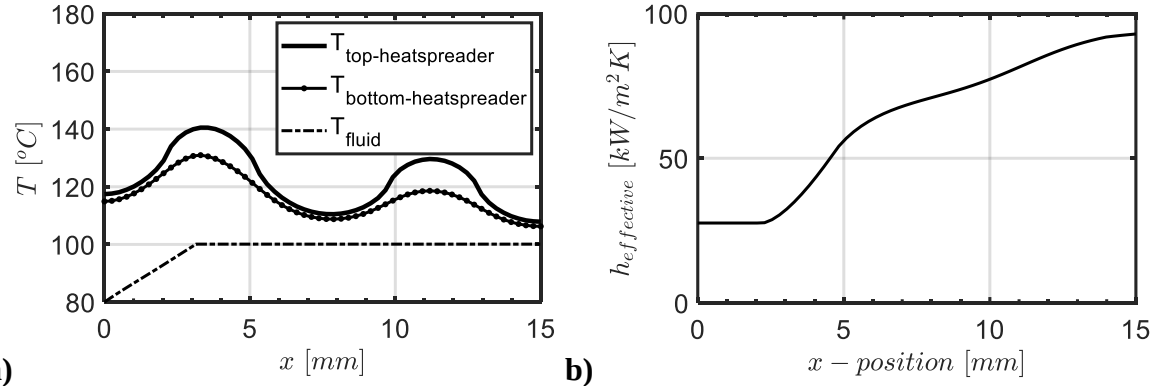

Figure 4. a) The temperature at the top and bottom of the heatspreader and fluid temperature. **b)** The effective heat transfer coefficient along the length of the channel.

To further illustrate the applicability of the model, the temperature on top of the heat spreader is plotted for various heat spreader thicknesses, see Figure 5a. If the heat spreader is too thin (0.2mm) the local heat flux just underneath the chip becomes very high (Figure 5b), since the heat cannot spread well enough. This leads to a high peak temperature (150℃), resulting in possible chip damage. A too high thickness (2.0mm) will spread the heat well but leads to a higher temperature (143℃) as well, because of an overall larger thickness of the heat spreader. The optimal thickness for this chip configuration is found to be around 1.0mm, at which the maximum temperature is the lowest (139℃). This example illustrates how to obtain the optimal dimensions for a chip cooling device. Similarly, the model can be comfortably used for other configurations.

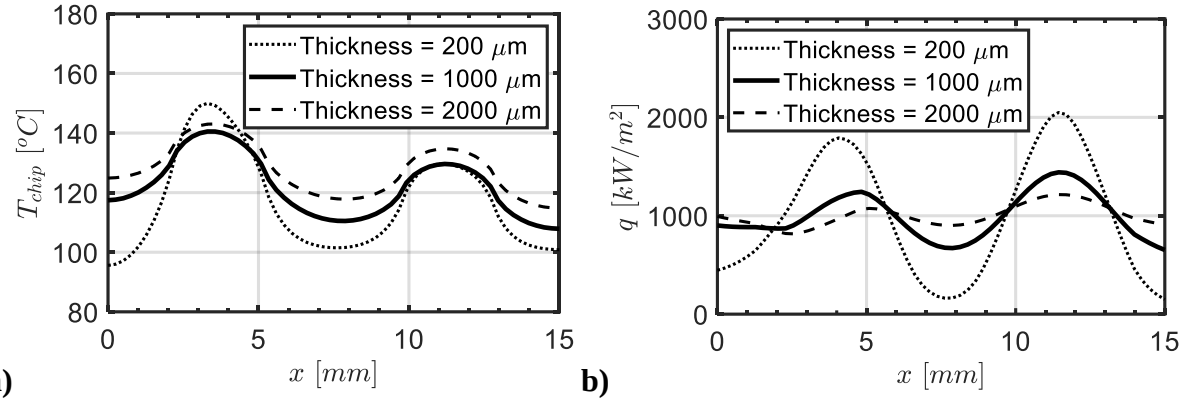

a) **b)**

Figure 5. a) The temperature at the top of the heatspreader for different heat spreader thicknesses. **b)** The heat flux into the cooling fluid, q_{bottom} , for different heat spreader thicknesses.

4. Conclusion

This paper demonstrates the importance of coupling a 2D temperature model to a microchannel flow boiling model. The coupling is required to accurately simulate the non-uniform heat flux along the cooling channel, as the local temperature of the heat spreader and the local properties of the fluid are dependent on one another. The applicability of the model is demonstrated using a simplified geometry. The model can be extended to incorporate more complex designs consisting of different materials. As such, the coupled model presented in this paper, warrants the opportunity to design an efficient cooling device, to reduce hot spots and achieve a low junction temperature.

References

[1] J. R. Thome, *Heat Transfer Engineering* 27, 9, 4–19, 2006.
[2] Z. Khattak, H. M. Ali, *Int. J. Heat. Mass. Tran.* 130, 141-161, 2019.
[3] Z. He, Y. Yan, Z. Zhang, *Energy* 216, 119223, 2021.
[4] T. G. Karayiannis, M. M. Mahmoud, *App. Thermal Engineering* 115, 1372-1397, 2017.
[5] C.M. Rops, J. E. Bullema, US2022028754 (A1), WO/2020/130837. 2020.
[6] K. P. Drummond, D. Back, M. D. Sinanis, D.B. Janes, D. Peroulis, J.A. Weibel, S. V. Garimella, *Int. J. Heat. Mass. Tran.* 117, 319-330, 2018.
[7] S. Kim, I. Mudawar, *Int. J. Heat. Mass. Tran.* 117, 55, 4, 958-970. 2012.
[8] J. R. Thome, V. Dupont, A. M. Jacobi. *Int. J. Heat. Mass. Tran.* 47, 3375-3385, 2004.
[9] P. V. O'Neil, *Beginning partial differential equations*, John Wiley and Sons, 1999.
[10] F. P. Incropera, D. P. Dewitt, *Fundamentals of heat and mass transfer*, John Wiley and Sons, New York, 144, 2006.